

The T-loop Extension of the Tomato Protein Kinase AvrPto-dependent Pto-interacting Protein 3 (Adi3) Directs Nuclear Localization for Suppression of Plant Cell Death^{*[5]}

Received for publication, February 23, 2010, and in revised form, April 5, 2010. Published, JBC Papers in Press, April 6, 2010, DOI 10.1074/jbc.M110.117416

María J. Ek-Ramos[‡], Julian Avila[‡], Cheng Cheng[‡], Gregory B. Martin^{§¶}, and Timothy P. Devarenne^{‡1}

From the [‡]Department of Biochemistry and Biophysics, Texas A&M University, College Station, Texas 77843, the [§]Boyce Thompson Institute for Plant Research, Ithaca, New York 14853, and the [¶]Department of Plant Pathology and Plant-Microbe Biology, Cornell University, Ithaca, New York 14853

In tomato (*Solanum lycopersicum*), resistance to *Pseudomonas syringae* pv. *tomato* is elicited by the interaction of the host Pto kinase with the pathogen effector protein AvrPto, which leads to various immune responses including localized cell death termed the hypersensitive response. The AGC kinase Adi3 functions to suppress host cell death and interacts with Pto only in the presence of AvrPto. The cell death suppression (CDS) activity of Adi3 requires phosphorylation by 3-phosphoinositide-dependent protein kinase 1 (Pdk1) and loss of Adi3 function is associated with the hypersensitive response cell death initiated by the Pto/AvrPto interaction. Here we studied the relationship between Adi3 cellular localization and its CDS activity. Adi3 is a nuclear-localized protein, and this localization is dictated by a nuclear localization signal found in the Adi3 T-loop extension, an ~80 amino acid insertion into the T-loop, or activation loop, which is phosphorylated for kinase activation. Nuclear localization of Adi3 is required for its CDS activity and loss of nuclear localization causes elimination of Adi3 CDS activity and induction of cell death. This nuclear localization of Adi3 is dependent on Ser-539 phosphorylation by Pdk1 and non-nuclear Adi3 is found in punctate structures throughout the cell. Our data support a model in which Pdk1 phosphorylation of Adi3 directs nuclear localization for CDS and that disruption of Adi3 nuclear localization may be a mechanism for induction of cell death such as that during the Pto/AvrPto interaction.

During the resistance response of plants to pathogens, programmed cell death (PCD)² occurs as part of the hypersensitive

response (HR), which functions to limit pathogen spread (1, 2). It has been over 100 years since the first description of the HR and its associated cell death (3). However, not until relatively recent times has the search for genes and pathways regulating PCD during the HR received much attention. This search has been difficult, but has identified several kinases and transcription factors involved in PCD (1, 4, 5) as well as lipid biosynthetic genes that produce lipid second messengers regulating PCD (6–9).

In tomato (*Solanum lycopersicum*), the causative agent of bacterial speck disease is *Pseudomonas syringae* pv. *tomato* (*Pst*). Interaction of the tomato resistance protein kinase Pto with the *Pst* effector protein AvrPto brings about the HR and resistance to *Pst* (10). Studies have been undertaken to identify genes involved in PCD associated with Pto-mediated HR and revealed a downstream MAP kinase, MAPKKK α , that functions in the induction of cell death during both resistance and susceptibility (11).

Another gene that was identified as a Pto-interacting protein was the tomato protein kinase Adi3, which only interacts with Pto in the presence of AvrPto (12). Subsequently, we have shown Adi3 to function as a negative regulator of plant cell death (13) and thus, it may be the functional homologue of PKB (aka Akt), a major PCD suppressor in mammals (13–15). Adi3 is phosphorylated by 3-phosphoinositide-dependent protein kinase-1 (Pdk1) at Ser-539, which is required for full Adi3 kinase activity and cell death suppression (CDS) ability (13). Mutation of Ser-539 to Asp is capable of mimicking this phosphorylation event, creating a constitutively active Adi3 capable of CDS (13). Adi3 cell death control can also be associated with MAPKKK α that is involved in Pto-mediate HR cell death (11, 13).

Adi3 is a member of the AGC kinase family, which is a conserved family of eukaryotic Ser/Thr protein kinases that regulate many basic cellular processes such as transcription, translation, cell growth, apoptosis, and cytoskeletal remodeling (16). In mammalian systems, AGC kinases affect downstream signaling components through direct mechanisms, including regulation of nuclear shuttling, activities of transcription factors (17), phosphorylation-dependent trafficking of signaling proteins (18), and chromatin remodeling (19). The cell death (apoptosis) regulator PKB is also an AGC kinase family member.

Little is known about the functions of plant AGC kinases. However, there has been several recent studies reported. As with mammalian systems, many plant AGC kinases are acti-

^{*} This work was supported by USDA-CSREES Grant 2007-35319-17832 (to G. B. M. and T. P. D.), USDA-AFRI Grant 2010-65108-20526 (to T. P. D.), and by Texas A&M University Dept. of Biochemistry and Biophysics start-up funds (to T. P. D.).

^[5] The on-line version of this article (available at <http://www.jbc.org>) contains supplemental Figs. S1–S5.

¹ To whom correspondence should be addressed. Tel.: 979-862-6509; Fax: 979-845-9274; E-mail: tpd8@tamu.edu.

² The abbreviations used are: PCD, plant cell death; Adi3, AvrPto-dependent Pto-interacting protein 3; AGC, cAMP-dependent protein kinase (PKA)/protein kinase G/protein kinase C (PKC) protein kinase family; CDS, cell death suppression; DIC, differential interference contrast image; eGFP, enhanced green fluorescent protein; HR, hypersensitive response; MBP, maltose-binding protein; Ndr kinase, nuclear Dbf2-related kinase; NES, nuclear exportation signal; NLS, nuclear localization signal; Pdk1, 3-phosphoinositide-dependent protein kinase-1; *Pst*, *P. syringae* pv. *tomato*; Xpo1, Exportin-1 (yeast CRM1-homolog); MES, 4-morpholineethanesulfonic acid.

vated by Pdk1 (13, 16, 20–23). *Arabidopsis* contains at least 39 AGC kinase family members (16, 21, 24) and some of their functions include blue-light signaling (25), root hair development (22, 26, 27), oxidative burst signaling (23, 27), and auxin signaling (24, 28). Group VIIIa AGC kinases (of which Adi3 is a member) are specific to plants and are mainly distinguished from mammalian kinases by a large 70–100 amino acid insertion in the activation loop, or T-loop, referred to as the T-loop extension (16). Similar, but much shorter (30–60 amino acids) T-loop extensions are also present in other AGC kinases such as the Ndr family of AGC kinases (29). In mammals and yeast, Ndr kinases regulate processes such as cell morphological changes, exit from mitosis, and apoptosis. The Ndr T-loop extension functions in cell localization and regulation of kinase activity (29–32). Very little is known about the function of the T-loop extension in plant AGC kinases. The T-loop extension of only two *Arabidopsis* group VIIIa AGC kinases have been studied and appear to contain cellular localization signals (21). However, the amino acid motifs within these T-loop extensions responsible for directing cellular localization have not been identified.

Here we show that the Adi3 T-loop extension is required for nuclear localization and that Adi3 nuclear localization is required for its CDS activity. Non-nuclear localization confines Adi3 to intracellular punctate membrane structures and a concomitant loss of CDS. These studies raise the possibility of restricting Adi3 nuclear localization as a means to induce plant PCD.

EXPERIMENTAL PROCEDURES

Plasmid Construction and Mutagenesis—The Adi3^{ΔT-loop} construct was created by producing an *Adi3* PCR fragment lacking the T-loop extension (bp 1369–1608). First, a PCR product containing *Adi3* bp 1336–1368 + 1609–2103 was synthesized and called fragment 1. Next another *Adi3* PCR product, fragment 2, from bp 1–1368 was produced that overlapped fragment 1. Both fragment 1 and 2 were then used as templates for overlapping PCR (33) with a 30-bp forward primer originating at *Adi3* bp 1 and a 27 bp reverse primer originating at *Adi3* bp 2103 to produce a PCR product lacking the T-loop extension. For bacterial expression, full-length tomato *Adi3* (13) and *Adi3*^{ΔT-loop} were PCR amplified and cloned into pMal-c2 (New England Biolabs). Mutations were created using site directed mutagenesis with Pfu Turbo (Stratagene). For protoplast expression, transient leaf expression, and subcellular localization studies, *Adi3*, *Adi3*^{ΔT-loop}, and other *Adi3* mutants were cloned into the BamHI/XbaI restriction sites of pTEX-*eGFP* to create N-terminal GFP fusions. For Agrobacterium-mediated transient expression, *35Spro:eGFP-Adi3* was EcoRI/HindIII digested from pTEX and cloned into the same sites of pCambia1300. For *GFP-NES/NLS* constructs, *eGFP* was PCR amplified with a *GFP*-specific forward primer and a reverse primer containing the *Adi3* NLS plus *GFP* (5'-CCGggattcCTAAGGCTTAGGTGTTTTTTCTTGCTCTTTTGAGGTTTGTATAGTTCATC-3'; BamHI lowercase; linker bold; *NLS* underlined, bp 1509–1542; *GFP* italics) for 3'-end fusion or with a *GFP*-specific reverse primer and a forward primer containing the *Adi3* NES plus *GFP* (5'-CCGgtaccATGCCTTTC-

TTGGACGATCTTTCAATCCGGATGCCAAGTAAAGGA-GAACAA-3'; KpnI lowercase; linkers bold; *NES* underlined, bp 373–490; *GFP* italics) for 5'-end fusion and cloned into the KpnI/BamHI restriction sites of pTEX.

The tomato exportin-1 (*Xpo1*) cDNA was cloned by a combination of methods. First, the *Arabidopsis Xpo1* cDNA sequence (34) (GenBankTM accession Y18469) was used to screen the tomato EST data base for contigs containing the tomato *Xpo1* cDNA. From this search, clone cTOF-19-M20 was identified as containing a partial tomato *Xpo1* cDNA lacking the first 1466 5' base pairs. A full-length cDNA (GenBankTM accession GU126514) was identified by cloning the 1466 5' base pairs by 5'-RACE and a full-length open reading frame amplified by RT/PCR using a forward primer based at the ATG start codon (5'-ATGGCGCGGAGAAGCTGAGA-3') and a reverse primer based at the TGA stop codon (5'-TCATGAATCCACCATTTCATC-3'). The resulting 3228-bp PCR product was cloned into the yeast two-hybrid bait vector pEG202, and protein interactions analyzed by yeast two-hybrid as previously described (13).

Protoplast Transient Expression and Cellular Fractionation—Protoplasts were isolated from leaves of 3-week-old PtoR or *prf-3* tomato plants and transformed with 20 μg of DNA for each construct as previously reported (13). Samples of transformed protoplasts were taken 16 h after transformation for protein expression determination, subcellular fractionation, and confocal microscopy. This time point was selected to minimize amount of dead cells, which is maximal at 24 h, to visualize expressed protein. Protoplast transformation efficiency was determined to be 80% by counting the number of GFP-positive protoplasts out of a total of 100 cells. Subcellular fractions were isolated using the following protocol: Total cell extract was obtained by gently shaking transformed protoplasts in 100 μl of Buffer A (10 mM MES-HCl pH 5.7, 1 M sucrose, 5 mM MgCl₂, 2 mM β-mercaptoethanol, 10 μl/ml phosphatase inhibitors (Sigma), 10 μl/ml proteinase inhibitors (Sigma), 10 μM MG-132, 0.2% Triton X-100). Nuclei were pelleted from total cell extract by centrifugation at 5,000 × g for 10 min at 4 °C followed by three washes with 100 μl of Buffer A and centrifugation at 5,000 × g for 10 min at 4 °C. Nuclei were lysed for SDS-PAGE analysis by vortexing in 30 μl of Buffer B (10 mM MES-HCl pH 5.7, 1 M sucrose, 5 mM MgCl₂, 2 mM β-mercaptoethanol, phosphatase inhibitors (Sigma), 10 μl/ml plant proteinase inhibitors (Sigma), 10 μM MG-132, 1% Triton X-100). The supernatant from nuclei pelleting was centrifuged at 100,000 × g for 1 h at 4 °C and the pellet used for the membrane fraction and the supernatant for the soluble fraction. Membrane proteins were solubilized by sonication in 30 μl of Buffer B. All fractions were separated by SDS-PAGE and analyzed by α-GFP (Santa Cruz Biotechnology) immunoblotting. Membrane fraction purity was determined using the Golgi marker soybean α-1, 2-mannosidase (GmMan1) tagged with m-Cherry (35) as expressed in protoplasts and analyzed by α-GFP immunoblotting. Purity of the nuclear fraction was determined by immunoblotting using α-histone H3 antibody provided by Dr. Mary Bryk, Texas A& M University. Subcellular fractionation analysis was done three independent times and the presented Western blots are representative of all experiments.

Adi3 Nuclear Localization Suppresses Cell Death

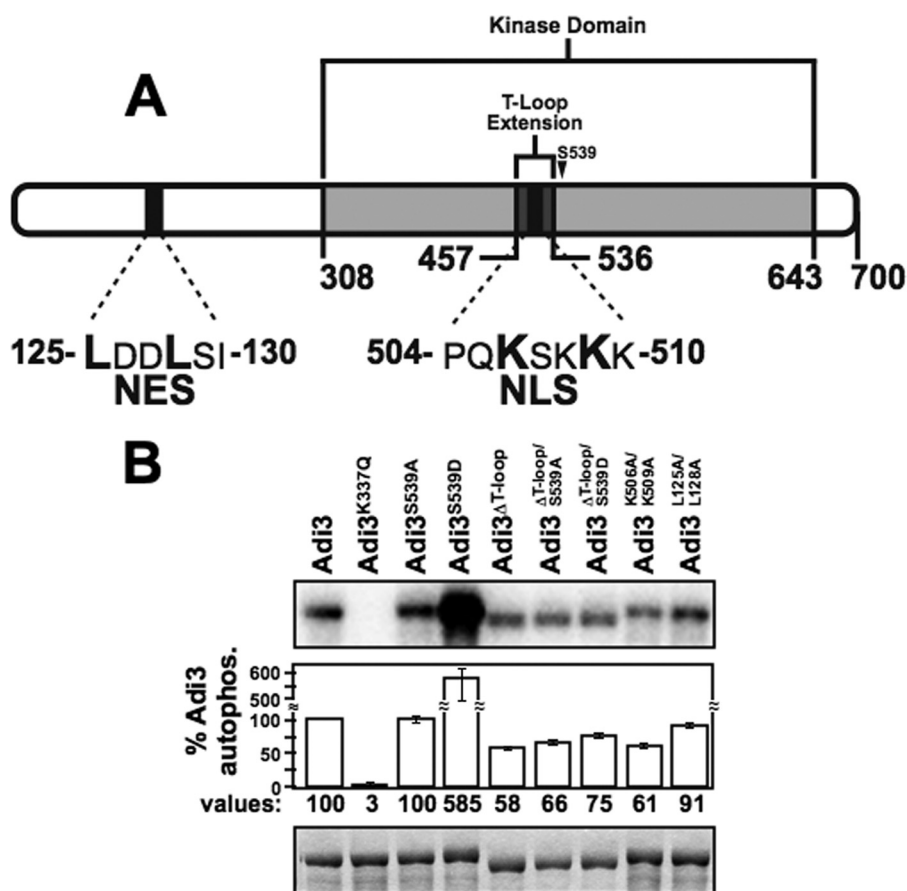


FIGURE 1. T-loop extension deletion effects on autophosphorylation activity of Adi3. *A*, Adi3 protein domains showing location of the T-loop extension and NLS and NES signals. *B*, kinase activity of Adi3 mutants tested by *in vitro* autophosphorylation assays. MBP-tagged proteins were expressed in *E. coli*, purified, and 5 μ g of each protein incubated with [γ -³²P]ATP in an *in vitro* kinase assay. Quantification software was used to normalize the autophosphorylation level to the protein levels for each sample. Values are reported as a percentage of wild-type Adi3 autophosphorylation and are the average of three independent experiments. Error bars are standard error. *Top panel*: kinase assay (phosphorimage). *Bottom panel*: assay input (Coomassie Blue-stained gel).

Confocal Microscopy—Tomato protoplasts, after 16 h of transformation and leaf sections taken from PtoR tomato leaves that were *Agrobacterium*-infiltrated, were imaged using an Olympus FV1000 confocal microscope at the Texas A&M University Microscopy and Imaging Center. Images were collected using system software FV10-ASW 1.6 with a 60 \times /1.2 water immersion objective in the XYZ scan mode (1.14 μ m/slice). Excitation and emission wavelengths were as follows: eGFP, 488 nm excitation, 507 nm emission; hoechst 33342 (Sigma), 343 nm excitation, 460 nm emission; and chlorophyll autofluorescence, 470 nm excitation, 680 nm emission. All cell localization analyses with confocal microscopy were carried out at least three independent times with a minimum of 30 protoplast cells and five leaf sections from three independently infiltrated leaves viewed each time. All confocal images are shown as Z-stacks and presented images are representative of typical cell localization for all proteins seen during independent experiments. For imaging protoplasts transformed with *GFP-Adi3* and *GFP-Adi3* mutants, the wavelength power was increased 2-fold in comparison to the power used for imaging protoplasts transformed with *GFP* alone.

Kinase Assays—*In vitro* kinase assays were done at least three independent times using purified *Escherichia coli*-expressed

MBP-tagged and immunoprecipitated GFP-tagged proteins as previously described (13).

AvrPto and Other Treatments—PtoR and *pfr-3* protoplasts expressing eGFP-Adi3 or other eGFP-Adi3 mutants for 14 h were transformed with pTEX-avrPto-FLAG. Samples were collected at 0.5, 1.5, 3, and 4 h for determination of cell viability. For nuclei staining and leptomycin B treatment, protoplasts expressing the indicated constructs for 14 h were treated with 10 μ M Hoechst 33342 for 2 h or 20 nM leptomycin B (Sigma) for 90 min followed by confocal microscopy imaging. All experiments were carried out a minimum of three times, and images presented are representative of the experiments.

Agrobacterium-mediated Transient Expression—*Agrobacterium tumefaciens* strain GV2260 was used for *Agrobacterium*-mediated transient expression in *Nicotiana benthamiana* and PtoR tomato leaves as previously reported (13). *Adi3* constructs were expressed from pCambia-1300 and *avrPto-FLAG* from pBTEX.

Cell Viability Measurements—Conductivity tests were carried out on 3 leaf discs (1-cm diameter) obtained from leaves transiently

expressing *Adi3* proteins. Disks were placed in 3 ml of dH₂O for 4 h with gentle shaking at room temperature and conductivity measured with an Acorn Con 5 meter (Oakton Instruments, Vernon Hills, IL). Cell death in leaves transiently expressing *Adi3* proteins was visualized by vacuum infiltrating 0.1% Evans blue into leaf disks followed by washing with dH₂O and depigmentation with Carnoy's solution (60% ethanol, 30% CHCl₃, 10% acetic acid). Protoplast cell viability was determined using Evans blue as previously reported (13). All cell viability assays were carried out a minimum of three independent times.

RESULTS

Adi3 Contains a Nuclear Localization Signal in the T-loop Extension and an N-terminal Nuclear Export Signal—A search of the *Adi3* protein sequence for cellular localization signals using the WoLF PSORT protein localization predictor (36) revealed a monopartite basic nuclear localization signal (NLS) in the *Adi3* T-loop extension from amino acids 504–510 (PQKSKKK, Fig. 1A). Additionally, the NESnet nuclear export signal (NES) search engine, identified a leucine-rich NES in the N-terminal region of *Adi3* from amino acids 125–130 (LDDL SI, Fig. 1A).

Because the Adi3 NLS is located in the T-loop extension, two different mutants to analyze contributions of this sequence to Adi3 function were generated as well as a mutant of the NES sequence. The Adi3 T-loop extension was deleted by overlapping PCR to generate the Adi3^{ΔT-loop} mutant, and the first (Lys-506) and third (Lys-509) Lys residue of the NLS were mutated to Ala creating the Adi3^{K506A/K509A} mutant. Mutation of equivalent Lys residues in NLS sequences similar to that in Adi3 is sufficient to prevent protein nuclear localization (37, 38). Similarly, in NES sequences analogous to that in Adi3, mutation of one or more Leu residues is sufficient to show nuclear accumulation of the protein (39). Thus, Leu-125 and Leu-128 were mutated to Ala to generate the Adi3^{L125A/L128A} mutant.

To determine if deletion of the Adi3 T-loop extension affects Adi3 kinase activity, autophosphorylation activity of the Adi3^{ΔT-loop} protein was tested and compared with known Adi3 autophosphorylation mutants. As seen previously, the S539D mutation produces a constitutively active Adi3 with greatly enhanced kinase activity (13) (Fig. 1B). Deletion of the T-loop extension (Adi3^{ΔT-loop}) reduced Adi3 autophosphorylation activity ~42%, which may be a cause of deleting the 79 amino acids of the T-loop extension within the catalytic kinase domain. Introduction of the S539D mutation into Adi3^{ΔT-loop} (Adi3^{ΔT-loop/S539D}) increased Adi3^{ΔT-loop} autophosphorylation by ~19% (Fig. 1B) indicating that mimicking Pdk1 phosphorylation of Adi3^{ΔT-loop} (Adi3^{ΔT-loop/S539D}) does not increase Adi3^{ΔT-loop} autophosphorylation activity to the extent of wild type. Interestingly, the NLS mutant (Adi3^{K506A/K509A}) had autophosphorylation activity close to that of Adi3^{ΔT-loop} (Fig. 1B) suggesting these Lys residues offer important structural features to Adi3 required for autophosphorylation activity. The NES mutant, Adi3^{L125A/L128A} did not drastically affect Adi3 autophosphorylation activity (Fig. 1B). The K337Q mutation (Adi3^{K337Q}) eliminates ATP binding and kinase activity in wild-type protein (13). Because the T-loop extension deletion and the NLS mutation affected Adi3 autophosphorylation activity, we next tested if these mutations had effects on Adi3 CDS activity and cellular localization.

In Vivo Expression Levels of GFP-Adi3 Expressed from the 35S Promoter and Functionality of the GFP-Adi3 Protein—Our Adi3 functional and localization studies use a GFP-Adi3 protein expressed from the cauliflower mosaic virus 35S promoter (*35Spro*). Use of the *35Spro* can lead to overexpression and accumulation of large amounts of protein, possibly leading to mislocalization. Thus, we analyzed the GFP-Adi3 protein levels in tomato protoplasts expressing *35Spro:GFP-Adi3* and compared this to the protein levels of two other proteins expressed from the *35Spro:AvrPto-BFP*, a *Pst* effector protein fused to BFP, and GFP alone. Western blot analysis indicated that the detection levels of GFP-Adi3 were very low and required 8 times and 40 times as much total protein to be detected compared with AvrPto-BFP or GFP, respectively (Fig. 2A). This suggests that GFP-Adi3 proteins do not reach levels that may cause problems in cellular localization analysis. In addition, we found one nonspecific band in our Western blot that could be detected only when high concentrations of total protein were used (*asterisk* in Fig. 2A and [supplemental Fig. S1](#)). This protein is larger than that of GFP alone suggesting it is not GFP and

indicating the presence of intact GFP-Adi3 as expressed in protoplasts. Additionally, the GFP-Adi3 protein used for subsequent localization and functional analyses was also fully kinase active as expected (Fig. 2B).

Ser-539 Phosphorylation and an Intact NLS Are Important for Adi3 CDS Activity—We used our Adi3 expressing protoplast system (13) to test different Adi3 kinase activity mutants for compromised cell death control (Fig. 2C). These assays make two premises. First, PCD is a process that is always “on” and there are proteins such as PKB and Adi3 that continually suppress PCD to prevent cell death (13–15). Loss of these proteins relieves suppression of PCD and initiates cell death as has been seen for PKB (40, 41) and we have seen for Adi3 (13). Second, overexpression of functionally compromised or constitutively active forms of PCD suppressor kinases will outcompete the endogenous protein, acting in a dominant negative or dominant manner, to induce or suppress cell death, respectively. This has been shown for PKB (42–46) and Adi3 (13). In our current assays, GFP-Adi3 proteins were expressed in protoplasts for 24 h and cell viability measured by Evans blue staining as we have previously done (13). These assays used protoplasts from *PtoR* tomato plants, which contain a functional *Pto* gene and show strong induction of HR cell death in response to the *Pst* effector protein AvrPto (10). For this reason, we used AvrPto expression as a positive control for strong cell death induction. Expression of wild-type Adi3 showed a moderate increase in cell viability over the vector alone (Fig. 2C) supporting its role in CDS (13). The kinase-inactive Adi3^{K337Q} showed a reduction in CDS and the constitutively active Adi3^{S539D} had increased CDS (Fig. 2C) further indicating that Adi3 kinase activity and Pdk1 phosphorylation (via the Pdk1 phosphorylation mimic) is required for Adi3 PCD control. Expression of Adi3^{ΔT-loop} showed a reduction in CDS similar to Adi3^{K337Q} (Fig. 2C). However, introduction of the phosphomimic S539D mutation (Adi3^{ΔT-loop/S539D}) was able to restore CDS activity for Adi3^{ΔT-loop} to near wild-type levels (Fig. 2C). Introduction of the nonphosphorylatable S539A mutation into Adi3^{ΔT-loop} (Adi3^{ΔT-loop/S539A}) showed a strong loss of CDS (Fig. 2C). The NLS mutant Adi3^{K506A/K509A} also showed loss of CDS equal to that of Adi3^{ΔT-loop} (Fig. 2C). The Adi3 NES mutant, Adi3^{L125A/L128A}, had increased CDS comparable to Adi3^{S539D} (Fig. 2C). These data would suggest that a functional Adi3 NLS is required for proper CDS and that mimicking the Pdk1 phosphorylation can restore CDS activity to nonfunctional NLS mutants.

Subcellular Distribution of Adi3^{ΔT-loop} Proteins—To analyze the effect on Adi3 subcellular localization due to the loss of the T-loop extension, subcellular fractions from protoplasts expressing GFP-Adi3 proteins for 16 h were analyzed by Western blot (Fig. 2D). The Adi3 and Adi3^{S539D} proteins showed similar localization in the nucleus and membrane fractions, while no protein was detected in the soluble fraction (Fig. 2D). This localization pattern of GFP-Adi3 was confirmed with Adi3 tagged with the small, 9-amino acid HA epitope ([supplemental Fig. S2A](#)) indicating the large GFP protein did not affect localization of the Adi3 protein. The Adi3^{ΔT-loop} protein showed strong localization to the membrane fraction and drastically reduced detection in the nuclear fraction (Fig. 2D)

Adi3 Nuclear Localization Suppresses Cell Death

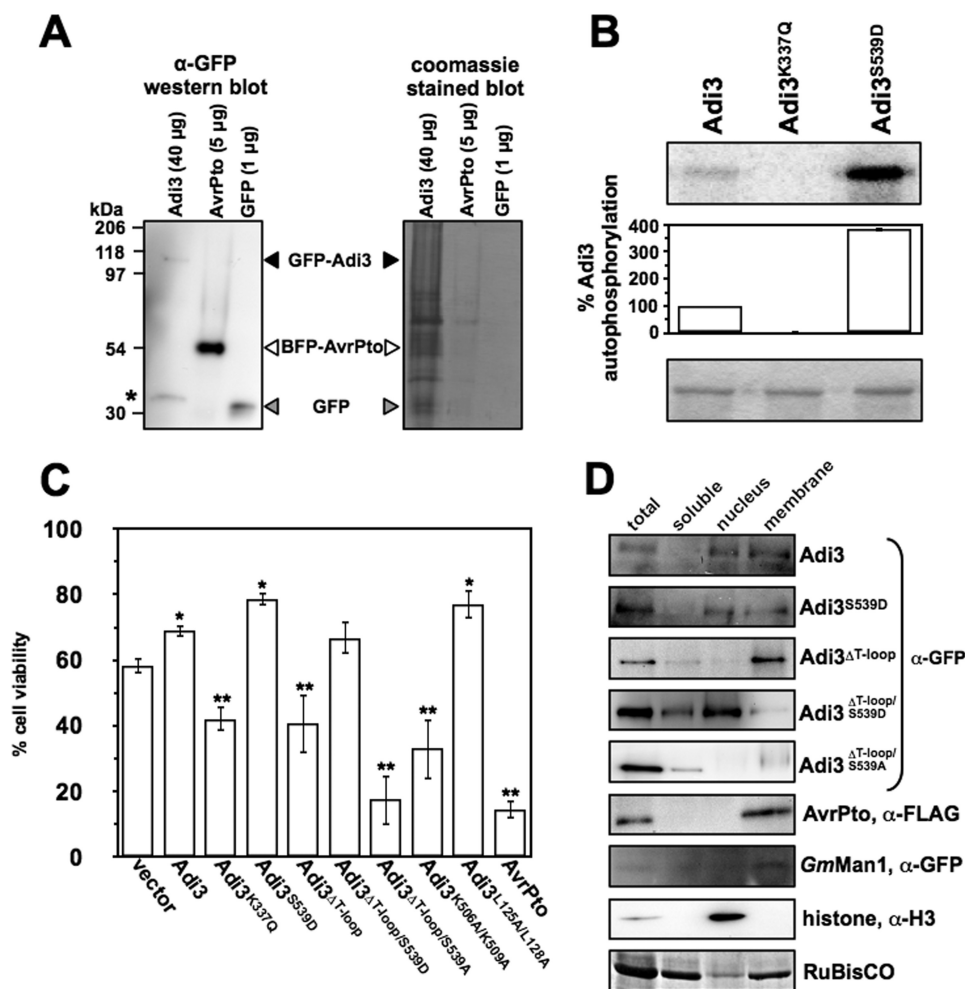


FIGURE 2. Cellular localization of GFP-Adi3 proteins regulates cell death suppression (CDS) activity. *A*, GFP-Adi3 protein expression levels under the 35S promoter. Tomato protoplasts were transformed with the indicated DNA constructs and protein expressed for 16 h followed by total protein extraction and α -GFP Western blot analysis. *B*, GFP-Adi3 autophosphorylation activity. Recombinant GFP-Adi3 protein was immunoprecipitated using α -GFP-agarose and tested in an *in vitro* kinase assay as in Fig. 1*B*. Values are reported as a percentage of wild-type Adi3 autophosphorylation and are average of three independent experiments. Error bars are standard error. *Top panel*: kinase assay (phosphorimage). *Bottom panel*: assay input (Coomassie Blue-stained gel). *C*, cell viability of protoplasts expressing GFP-Adi3 plus NLS and NES mutants. Tomato protoplasts expressing the indicated proteins for 24 h were analyzed for cell viability by Evans Blue staining to identify dead cells. Data represent the average of five independent experiments. Error bars are standard error. *One asterisk* and *two asterisks* indicate significant increase or decrease, respectively, in cell viability compared with vector-only expression (Student's *t* test, $p < 0.05$). *D*, subcellular distribution of GFP-Adi3 proteins. The indicated proteins were expressed for 16 h in tomato protoplasts followed by subcellular fractionation and Western blot with the indicated antibodies. Markers used: membrane, AvrPto-FLAG (73) and soy bean α -1,2-mannosidase (*GmMan1*)-mCherry (35); nuclei, histone H3; soluble fraction and loading control, RuBisCo (Coomassie Blue stain of membrane). Western blots are representative of three independent experiments.

indicating a lack of a functional NLS in the Adi3^{ΔT-loop} protein. Introduction of the S539D mutation (Adi3^{ΔT-loop/S539D}) caused a substantial shift of the Adi3^{ΔT-loop} protein to the nuclear fraction and reduction in membrane localization (Fig. 2*D*). The Adi3^{ΔT-loop/S539A} protein was not found in the nuclear fraction but was detectable in the membrane fraction only as a high molecular weight smear, suggesting post-translational modification (Fig. 2*D*). These data indicate that the Adi3 NLS in the T-loop extension directs nuclear localization and that mimicking Pdk1 phosphorylation of Adi3 without the T-loop extension (Adi3^{ΔT-loop/S539D}) can redirect the protein to the nucleus. Taken together with the CDS assays (Fig. 2*C*), these data suggest that loss of Adi3 nuclear localization (deletion of T-loop

extension or NLS mutant) impairs the ability of Adi3 to suppress cell death. Restoring nuclear localization (S539D introduction into Adi3^{ΔT-loop}) is capable of restoring Adi3 CDS. Additionally, our data support our earlier findings that overexpression of non-functional mutant forms of Adi3 act in a dominant negative manner with regard to the endogenous Adi3 protein (13).

Confirmation of Adi3 Nuclear Localization—To confirm Adi3 nuclear localization, GFP-Adi3 expressing protoplasts were treated with the nuclear export inhibitor leptomycin B, which restricts nuclear/cytoplasmic shuttling proteins to the nucleus (47, 48). The protoplasts were also treated with the DNA stain Hoechst 33342 to identify nuclei (49) followed by confocal microscopy imaging of the GFP and Hoechst 33342 signals. The results showed that leptomycin B treatment reduced cytoplasmic GFP-Adi3 and restricted the protein to the nucleus (Fig. 3*A*). We also cloned the nuclear export protein Exportin-1 (Xpo1), which binds leucine-rich NESs (34) and showed that Adi3 interacts with Xpo1 in a yeast two-hybrid assay (Fig. 3*B*). The functionality of the Adi3 NLS was also confirmed by fusing the NLS to the C terminus of GFP (GFP-NLS) and analyzing for nuclear accumulation of GFP. The protein was expressed in tomato protoplasts treated with hoechst 33342 for nucleus identification and cellular localization viewed by confocal microscopy. Protein expression was confirmed by α -GFP Western blot

(Fig. 3*D*). GFP-NLS protein localization was reduced in the cytoplasm, but retained in the nucleus suggesting the Adi3 NLS is a functional nuclear localization signal (Fig. 3*C*). A similar analysis was carried out with the Adi3 NES sequence, which was fused to the N terminus of GFP (NES-GFP). If the NES is functional, NES-GFP protein should accumulate in the cytoplasm. However, the Adi3 NES was incapable of reducing GFP nuclear localization (Fig. 3*C*) indicating the Adi3 NES may be a weak export signal unable to maintain nuclear exclusion of the small GFP protein, which can freely enter the nucleus (50, 51).

Adi3 Nuclear Localization Is Required for PCD Suppression in Tomato and Tobacco Leaves—Because Adi3 NLS loss, either by deletion of the T-loop extension or NLS mutation, causes

Adi3 Nuclear Localization Suppresses Cell Death

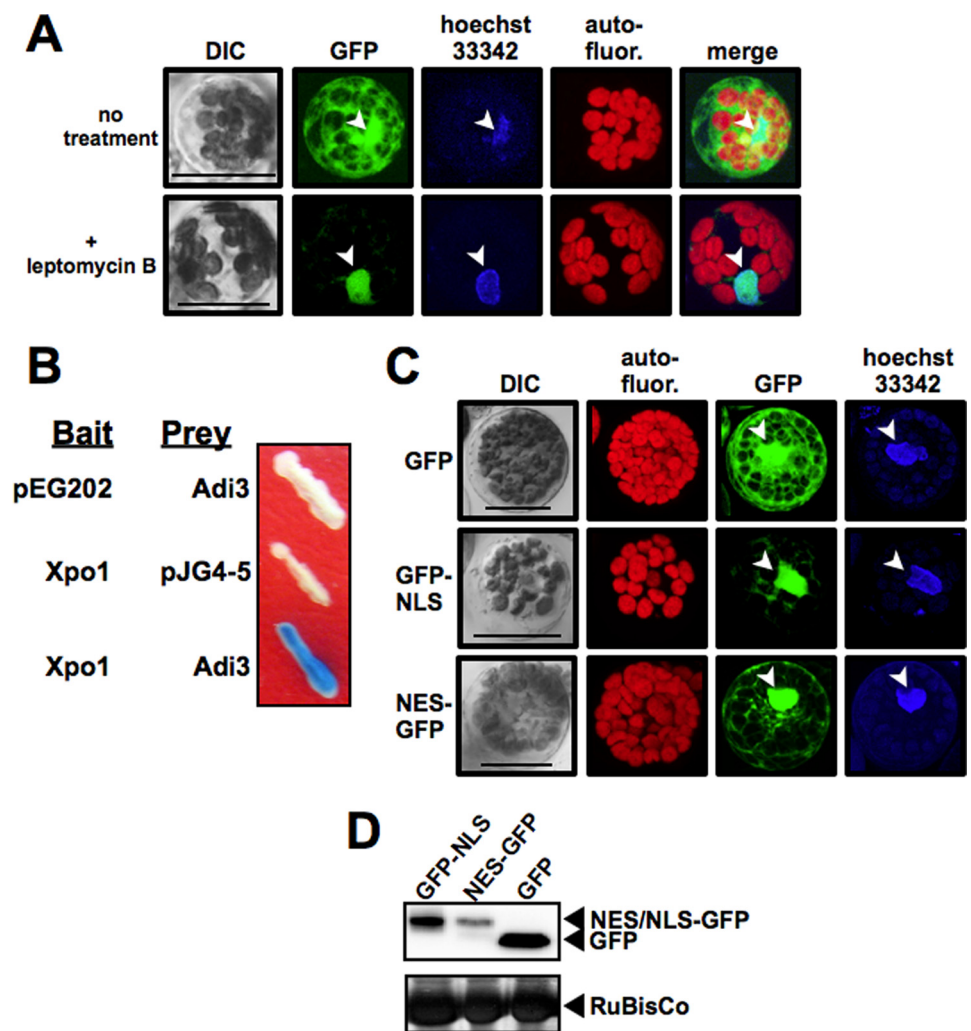


FIGURE 3. Adi3 contains a functional NLS. *A*, leptomycin B treatment. Tomato protoplasts expressing GFP-Adi3 for 14 h were incubated with 20 nM leptomycin B for 90 min followed by incubation with 10 μ M Hoechst 33342 for 2 h and visualized by confocal microscopy. *Merge*, overlay of GFP, Hoechst 33342, and autofluorescence images. *Bar*, 20 μ m; *arrowhead*, nucleus. *B*, Adi3 interaction with Xpo1. Xpo1 from tomato was cloned and tested for yeast two-hybrid interaction with Adi3 in the LexA system. *C*, functional analysis of Adi3 NES and NLS. The indicated GFP fusion proteins were expressed in tomato protoplasts for 14 h, treated with 10 μ M Hoechst 33342 for 2 h, and visualized by confocal microscopy. *Bar*, 20 μ m; *arrowhead*, nucleus. *D*, expression of GFP-NLS and NES fusion proteins in tomato protoplasts as detected by α -GFP Western blot.

Adi3 to have compromised PCD control in protoplasts, functionality of GFP-Adi3 and GFP-Adi3 ^{Δ T-loop} proteins in leaf tissue was analyzed utilizing *Agrobacterium*-mediated transient expression in tomato (Fig. 4A) and *N. benthamiana* (Fig. 4B). As with our protoplast functionality assays (Fig. 2C), we used PtoR tomato plants, which produce strong HR cell death in response to the *Pst* effector AvrPto (10). *N. benthamiana* plants also produce HR cell death in response to AvrPto (10). Thus, expression of AvrPto-FLAG was used as a strong cell death inducer positive control (Fig. 4, A and B). In the assays, leaves (tomato) or leaf disks (*N. benthamiana*) were taken at 12, 24, and 48 h after *Agrobacterium* infiltration, stained with Evans blue to identify dead cells, depigmented, and photographed. Protein expression in leaf tissue was confirmed by α -GFP and α -FLAG Western blot (Fig. 4C). In both tomato and *N. benthamiana*, expression of Adi3 showed no loss of CDS (Fig. 4, A and B). The Adi3 ^{Δ T-loop} protein showed a loss of CDS by 24 h after infiltration in tomato (Fig. 4A)

and 48 h in *N. benthamiana* (Fig. 4B). Expression of Adi3 ^{Δ T-loop/S539D} was capable of restoring CDS to wild-type levels in both tomato and *N. benthamiana*, while the expression of Adi3 ^{Δ T-loop/S539A} caused a very strong loss of CDS nearly equivalent to that of AvrPto (Fig. 4, A and B). This would suggest that Adi3 nuclear localization driven by mimicking Pdk1 phosphorylation of Ser-539 is required for CDS.

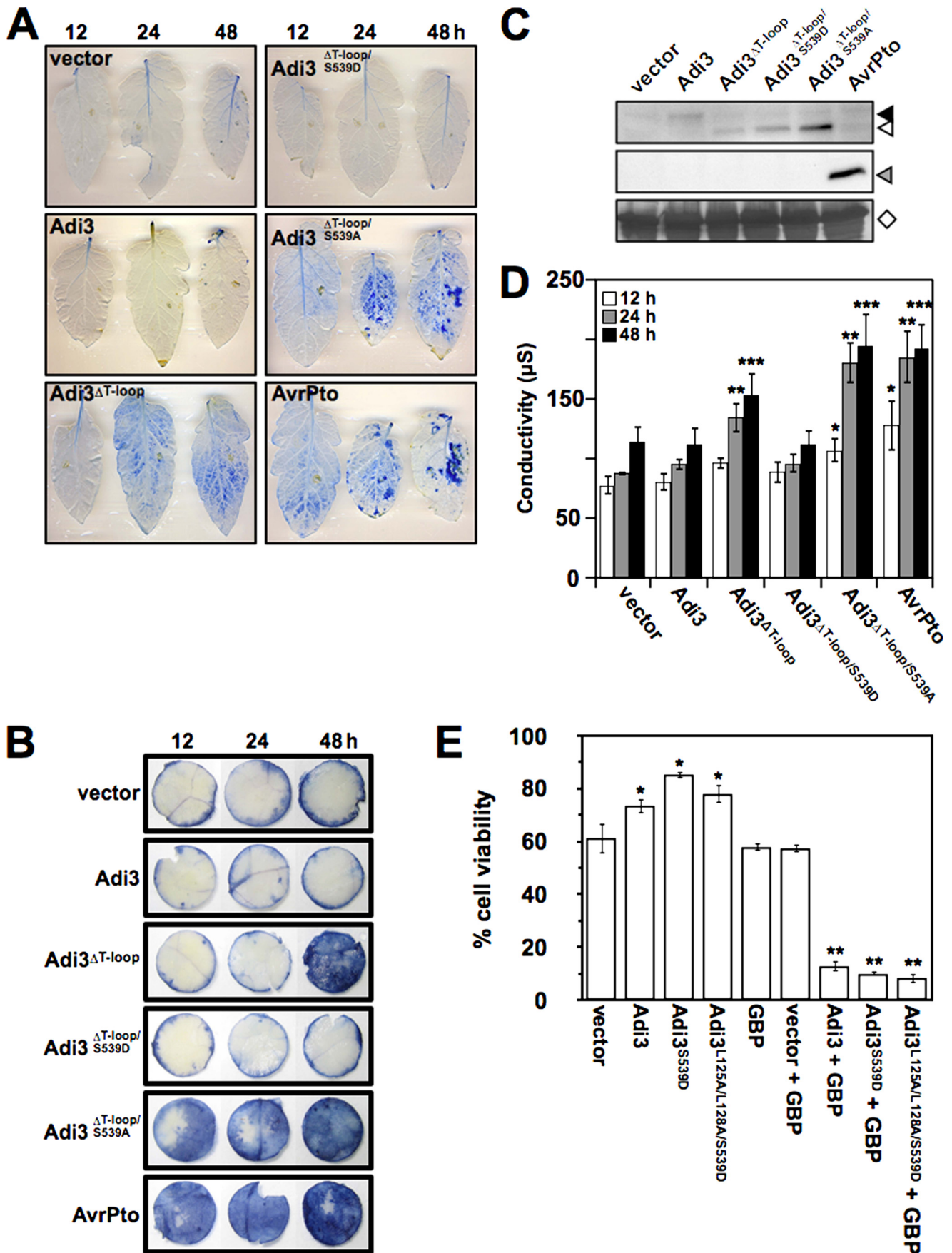
A reliable assessment of plant cell death is to measure cell ion leakage from leaf disks by measuring conductivity of a surrounding solution (52). Cell death control in leaf disks from Fig. 4B was analyzed by conductivity (Fig. 4D). The results matched the visualization of cell death seen with Evans blue staining; Adi3 ^{Δ T-loop} and Adi3 ^{Δ T-loop/S539A} were unable to suppress cell death, with Adi3 ^{Δ T-loop/S539A} showing the strongest loss (Fig. 4D). The Adi3 ^{Δ T-loop/S539D} protein had restored ability to suppress cell death (Fig. 4D). These CDS assays using intact leaves confirm the results seen in our protoplast system (Fig. 1C) and confirms that the protoplast system is a reliable platform for assessing Adi3 function.

As a further confirmation that nuclear Adi3 is required for its CDS activity, we coexpressed GFP-Adi3 in PtoR tomato protoplasts with a GFP-binding protein (GBP) for 16 h and analyzed for loss of Adi3 CDS

by Evans blue-stained dead cells. This GBP protein has been shown in plants to effectively bind GFP fusion proteins *in vivo* and disrupt the function of nuclear-localized cell death-regulating proteins by restricting them to the cytoplasm (53). Expression of GBP alone did not alter cell viability (Fig. 4E). However, coexpression of GBP with Adi3, Adi3^{S539D}, or Adi3^{L125A/L128A/S539D} showed a strong loss of Adi3 CDS activity (Fig. 4E) further indicating a nuclear-localized Adi3 is required for full CDS. A reduction in the nuclear localization of the GFP-Adi3 proteins expressed with GBP was confirmed by α -GFP Western blot (supplemental Fig. S2B).

Deletion of the T-loop Extension Causes Localization of Adi3 to Punctate Cellular Structures—To confirm subcellular fractionation results (Fig. 2D), confocal microscopy was used to visualize the localization of GFP-Adi3 and GFP-Adi3 NLS mutants in *Agrobacterium*-infiltrated intact tomato leaf mesophyll cells (Fig. 5A) and tomato mesophyll protoplasts (Fig. 5B). Protein expression of GFP-Adi3 proteins were confirmed by

Adi3 Nuclear Localization Suppresses Cell Death



α -GFP Western blot analysis (Fig. 5C). Both systems showed similar results. Adi3 wild type appeared to be localized throughout the entire cell, while GFP-Adi3 ^{Δ T-loop} protein was localized to punctate structures throughout the cell (Fig. 5, A and B). Localization of the GFP-Adi3 ^{Δ T-loop} protein appears to be regulated by the mimicking phosphorylation status of the Pdk1 phosphorylation site, Ser-539. Introduction of the S539D mutation into the Adi3 ^{Δ T-loop} protein decreased punctate structure localization and directed some protein to the nucleus (Fig. 5, A and B), which was also seen in the subcellular fractionation (Fig. 2D). Introduction of the S539A mutation caused an increase in the number of Adi3 ^{Δ T-loop} punctate structures with no nuclear localization (Fig. 5B). Expression of the Adi3^{K506A/K509A} protein also showed localization to punctate structures similar to the Adi3 ^{Δ T-loop} protein (Fig. 5, A and B). The number of GFP-Adi3 ^{Δ T-loop} punctate structures seen in protoplasts were quantified for each mutant and showed that expression of GFP-Adi3 ^{Δ T-loop/S539A} is located to the most punctate structures (supplemental Fig. S3). Because the Adi3 ^{Δ T-loop/S539A} protein has very strong loss of CDS activity and a high amount of localization to punctate cellular structures, there appears to be a strong correlation between the number of punctate structures and induction of PCD. Several attempts to identify these punctate structures have not yielded positive results. However, the Adi3 ^{Δ T-loop} proteins do appear to be enriched in the membrane fraction (Fig. 2D) suggesting the punctate structures are an intracellular membrane system.

Nuclear-localized Adi3 Can Suppress AvrPto-induced Cell Death—To test our findings that nuclear-localized Adi3 can suppress cell death, we tested the ability of constitutively active and nuclear forms of Adi3 to suppress the induction of cell death caused by AvrPto. PtoR tomato protoplasts expressing GFP alone (vector) or wild-type and mutant GFP-Adi3 proteins for 14 h were transformed with BFP-AvrPto or a water control and cell death measured with Evans Blue over a 4-h time period. Expression of Adi3 and AvrPto were confirmed by α -GFP Western blot (supplemental Fig. S4). Cell death was strongly induced by expression of AvrPto alone as compared with GFP expression only (Fig. 6A, compare first and last column of each time point). Wild-type Adi3 was capable of suppressing this cell death induced by AvrPto at 0.5 h and to a small level at 1.5 h after AvrPto expression (Fig. 6A, compare second and last column of each time point). The constitutively active Adi3^{S539D} and the constitutively nuclear-localized and active Adi3^{L125A/L128A/S539D} were both able to very strongly suppress AvrPto-induced cell death up to 4 h after AvrPto expression

(Fig. 6A, compare fourth and fifth column with last column of each time point). Interestingly, kinase-inactive Adi3^{K337Q} was able to suppress AvrPto-induced cell death at 0.5 h after AvrPto expression (Fig. 6A, compare third and last column of each time point). These assays were also carried out in protoplasts from *prf-3* tomato plants which have a mutation in the *Prf* gene (54, 55). This gene is required for Pto-mediated cell death in response to AvrPto, and cell death is not induced in *prf-3* plants when treated with AvrPto (10, 54, 55). As expected, cell viability was maintained at or near the GFP alone control in all combinations of Adi3 and AvrPto in *prf-3* protoplasts (Fig. 6B).

We also tested the ability of Adi3 to suppress non-pathogen induced forms of cell death in yeast, such as the cell death induced by H₂O₂ (56). Expression of GFP-Adi3 in yeast was capable of reducing the cell death induced by H₂O₂ (supplemental Fig. S5) suggesting the Adi3 CDS mechanism is highly conserved in eukaryotes. In these assays the *Pst* effector protein AvrPtoB was used as a positive control for H₂O₂ CDS (57).

Taken together, these data confirm that nuclear-localized Adi3 is capable of suppressing cell death and that the function of overexpressed, active forms of Adi3 can be analyzed *in vivo* because they outcompete endogenous Adi3 protein as we have seen previously (13). Our *in vivo* functional studies, which use GFP-Adi3 proteins, also suggest that the localization of the GFP-Adi3 proteins is correct since the CDS activity of these GFP-Adi3 proteins matches predicted Adi3 function and that previously seen for constitutively active Adi3^{S539D} (13).

DISCUSSION

Identification of plant proteins that regulate PCD has been difficult and yielded few results as compared with mammalian systems (1, 4, 5, 58). However, several MAP kinases and transcription factors have been identified that regulate plant PCD (11, 59–64). Additionally, a few homologues of mammalian PCD regulators have been found in plant systems (65). Given the important roles of PCD in plant development and pathogen interactions, identification, and characterization of such proteins is critical for understanding how plant PCD functions. We identified the protein kinases Adi3 and Pdk1 as negative regulators of plant PCD (13). Our studies here firmly place Adi3 as a suppressor of PCD in tomato and provide insights into the role of cellular localization in controlling Adi3 CDS activity that are strikingly similar to the apoptosis suppressing function of PKB in mammalian systems. Because Adi3-like sequences are found

FIGURE 4. Nuclear-localized Adi3 is required for CDS. A, CDS loss in tomato leaves expressing Adi3 ^{Δ T-loop} proteins. *Agrobacterium tumefaciens*-mediated transient expression of GFP-Adi3 and GFP-Adi3 ^{Δ T-loop} proteins was carried out in PtoR tomato leaves. After indicated times, whole leaves were Evans Blue stained, depigmented, and photographed. AvrPto-FLAG was used as positive control for cell death. B, CDS loss in *N. benthamiana* leaves expressing Adi3 ^{Δ T-loop} proteins. *Agrobacterium*-mediated transient expression of GFP-Adi3 and GFP-Adi3 ^{Δ T-loop} proteins was carried out in *N. benthamiana* leaves. After indicated times, 1 cm in diameter leaf disks were treated as in A for visualization of induced cell death. C, Western blot of proteins expressed in tomato leaves. Total protein extract was obtained from leaves transiently expressing GFP-Adi3 and GFP-Adi3 ^{Δ T-loop} proteins and Western analysis carried out using α -GFP (top panel) and α -FLAG (bottom panel) antibodies. Filled triangle, GFP-Adi3; open triangle, GFP-Adi3 ^{Δ T-loop} proteins; gray triangle, AvrPto-Flag; open diamond, RuBisCo loading control. D, ion leakage as indication of cell death induction. Conductivity tests were carried out on three 1-cm diameter disks from tomato leaves transiently expressing GFP-Adi3 and GFP-Adi3 ^{Δ T-loop} proteins at indicated times. Values are the average of three independent experiments. Error bars are standard error. One asterisk, two asterisks, and three asterisks indicate significant increase in ion leakage at 12, 24, and 48 h, respectively, compared with vector only expression at those time points (*t* test, *p* < 0.05). E, restriction of GFP-Adi3 to cytoplasm by the GFP-binding protein eliminates Adi3 CDS. The indicated combinations of GFP-Adi3 and GBP were expressed in tomato protoplasts for 16 h and observed for cell death using Evans blue staining. All data represent average of three independent experiments. Error bars are standard error. One asterisk and two asterisks indicate significant increase or decrease, respectively, in cell viability compared with vector-only expression (*t* test, *p* < 0.05).

Adi3 Nuclear Localization Suppresses Cell Death

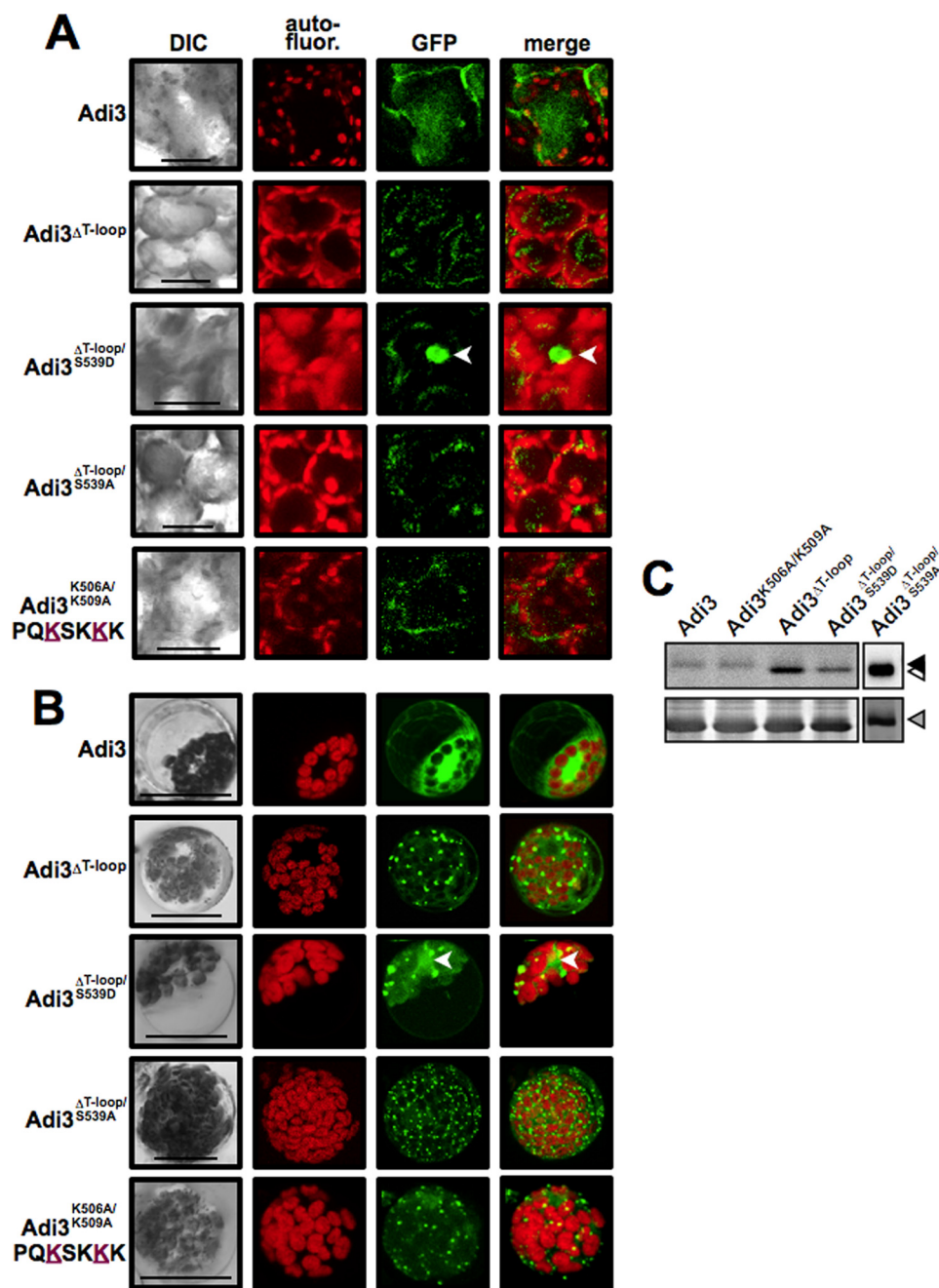


FIGURE 5. Adi3 NLS mutants are located in punctate cellular structures. *A*, localization of GFP-Adi3 proteins in intact PtoR tomato leaf mesophyll cells. After *Agrobacterium*-mediated transient expression for 48 h (GFP-Adi3), 24 h (GFP-Adi3^{ΔT-loop}; GFP-Adi3^{ΔT-loop/S539D}), or 12 h (GFP-Adi3^{ΔT-loop/S539A}; GFP-Adi3^{K506A/K509A}), leaf sections were cut from 3 different leaves and visualized by confocal microscopy. Images are representative of three independent experiments. *Merge*, overlay of GFP and autofluorescence images. *Bar*, 20 μm; *arrowhead*, nucleus. *B*, localization of GFP-Adi3 proteins in PtoR tomato protoplasts. The indicated GFP-Adi3 proteins were expressed in protoplasts for 16 h and visualized by confocal microscopy. Labeling as in *A*. *C*, Western blot using α-GFP antibody on total protein from expression of the indicated GFP-Adi3 proteins. *Filled triangle*, GFP-Adi3; *open triangle*, GFP-Adi3^{ΔT-loop} proteins; *gray triangle*, RuBisCo loading control (Coomassie Blue-stained membrane).

in many plants (*Arabidopsis*, rice, corn), it is possible that PCD is regulated in a similar manner in most plants.

The NLS in the Adi3 T-loop Extension Directs Nuclear Localization—Our data show that the Adi3 T-loop extension contains an NLS that is required for nuclear localization. Other studies have suggested that this T-loop extension of plant AGC kinases also functions in determining cellular localization. The

T-loop extension of the plant AGC kinases PID and AGC1–7 directs these proteins to the plasma membrane and cytoplasm, respectively (21). Nuclear localization of two other plant VIIIa AGC kinases, KIPK and WAG1, has been shown, but the requirement of the T-loop extension has not been reported (21). The Ndr family of mammalian AGC kinases also contains T-loop extensions similar to plant VIIIa AGC kinases. The extension encodes an NLS for Ndr1, but it appears to inhibit autophosphorylation in other Ndr kinases (29–32). The Adi3 T-loop extension does not appear to be an inhibitor of autophosphorylation. Sequence identity and amino acid length of both mammalian and plant AGC kinase T-loop extensions are quite variable. However, they all contain a stretch of basic amino acids near the C-terminal end of the extension that appears to give functionality to the extension (21, 29). In Ndr1 (31) and Adi3, these basic amino acids encode the NLS and in other Ndr kinases they are responsible for autophosphorylation inhibition (32). Examination of other plant VIIIa AGC kinase T-loop extensions is required to determine if these basic amino acids are required for cellular localization or kinase activity.

Pdk1 Phosphorylation of Adi3 Is Required for Nuclear Localization and CDS—The presented results indicate that in addition to phosphorylation of Adi3 at Ser-539 for activation of kinase activity, mimicking Pdk1-mediated phosphorylation at Ser-539 is sufficient for Adi3 nuclear localization (Figs. 2*D* and 5, *A* and *B*). Interestingly, the S539D mutation can alter localization of the Adi3^{ΔT-loop} protein from punctate structures to the nucleus even though this protein lacks the identified NLS (Fig. 5, *A* and *B*), suggest-

ing the S539D phosphorylation mimic may produce a conformational change sufficient for interaction with nuclear import machinery or exposure of a nonconsensus NLS. Pdk1-dependent nuclear localization of plant AGC kinases has not been reported. However, the mammalian AGC kinase PKB is phosphorylated at the plasma membrane on Thr-308 by Pdk1, which mobilizes PKB to the nucleus (14, 66, 67).

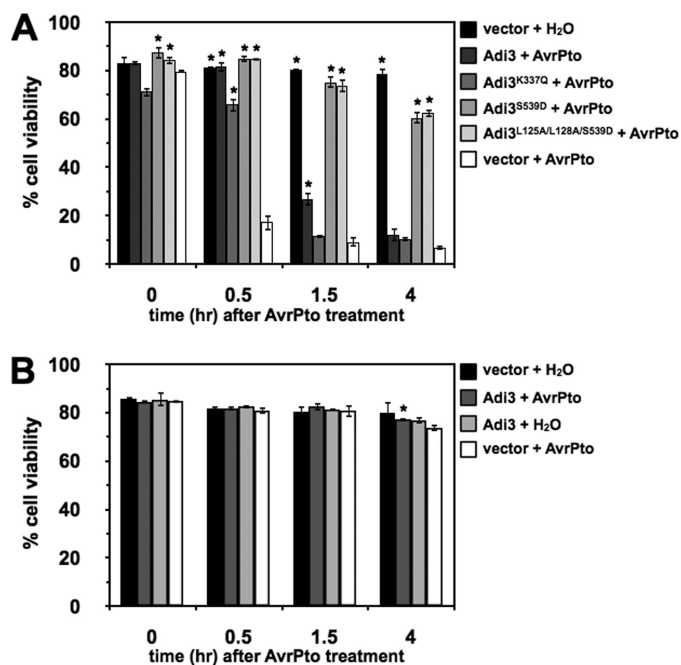


FIGURE 6. Nuclear-localized Adi3 protects against AvrPto-induced cell death. *A*, PtoR tomato protoplasts or *B*, *pfr-3* tomato protoplasts were transformed with indicated GFP-Adi3 constructs, proteins were expressed for 14 h and transformed with an *avrPto* construct, samples were taken at the indicated times, and cell viability determined by Evans Blue staining. Graphs represent the average of three independent experiments. Error bars are standard error. One asterisk indicates significant increase in cell viability compared with AvrPto only expression within each time point (Student's *t* test, $p < 0.05$).

Mimicking Pdk1 phosphorylation of Adi3 Ser-539 is also required for CDS as indicated by restoration of CDS to the $\text{Adi3}^{\Delta\text{T-loop/S539D}}$ protein and strong loss of CDS for $\text{Adi3}^{\Delta\text{T-loop/S539A}}$ (Figs. 2C and 4, A, B, D) as well as the ability of $\text{Adi3}^{\text{S539D}}$ and $\text{Adi3}^{\text{L125A/L128A/S539D}}$ to suppress AvrPto-induced cell death (Fig. 6A). This is similar to Pdk1-phosphorylated, activated, and nuclear-localized PKB, which can phosphorylate nuclear substrates to suppress cell death (67–71). Interestingly, the S539D mutation does not increase $\text{Adi3}^{\Delta\text{T-loop}}$ kinase activity to the level of wild-type Adi3 (Fig. 1B) even though $\text{Adi3}^{\Delta\text{T-loop/S539D}}$ is capable of CDS, suggesting full autophosphorylation activity is not required for complete Adi3 CDS and that one mechanism by which Adi3 suppresses cell death may be protein interaction for functional inhibition independent of full kinase activity. This is supported by the finding that the kinase-inactive $\text{Adi3}^{\text{K337Q}}$ is capable of limited CDS (Fig. 6A). From our results a picture is evolving of a Pdk1/Adi3 kinase signaling cascade for suppressing cell death that is similar to mammalian Pdk1/PKB; Pdk1 phosphorylation of Ser-539 activates Adi3 kinase activity, which is sufficient to direct nuclear localization and is required for CDS activity.

A Model for Adi3 Function in Cell Death Control—Based on our results presented here and previous studies (13) we suggest a model of Adi3 function in PCD regulation. We have shown that the Pdk1-Adi3 interaction is constitutive (13) and most likely takes place at the plasma membrane because that is where Pdk1 is known to activate substrates (72). Mimicking phosphorylation of Adi3 Ser-539 by Pdk1 drives Adi3 nuclear localization where it functions to suppress PCD. Loss of Adi3 nuclear local-

ization through deletion of the T-loop extension or NLS mutation directs Adi3 to intracellular punctate structures where it no longer has CDS activity. These punctate structures appear to be an intracellular membrane system. This model, and the fact that Adi3 interacts with Pto and AvrPto (12, 13), raises the possibility that the induction of HR cell death during the pathogen resistance response is mediated by redirecting Adi3 from the nucleus to the punctate membrane structures seen here. This would inactivate Adi3 and induce PCD. In the future, it will be important to determine exactly how Adi3 is being mobilized to the nucleus and how this localization is regulated under pathogen-challenged situations. Additionally, it will be essential to identify the punctate membrane structures to which non-nuclear Adi3 is located, as well as to identify nuclear Adi3 substrates for CDS.

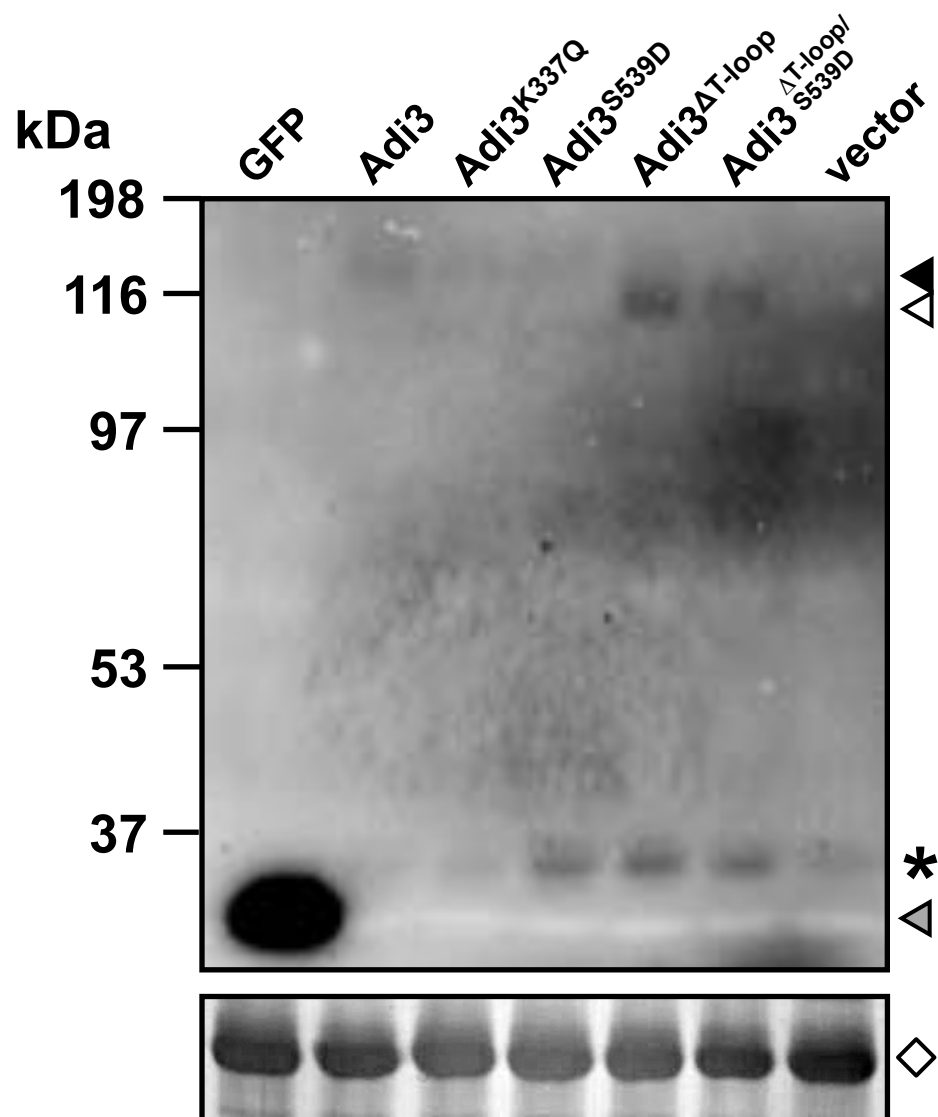
Acknowledgments—We thank Dr. Stan Vitha of the Texas A&M Microscopy and Imaging Center for assistance and critical advice with confocal imaging and members of the Devarenne Laboratory for comments and constructive discussions. The eBFP2 construct was kindly provided by Michael W. Davidson, Florida State University. The GFP-binding protein construct was kindly provided by Sophien Kamoun, The Sainsbury Laboratory.

REFERENCES

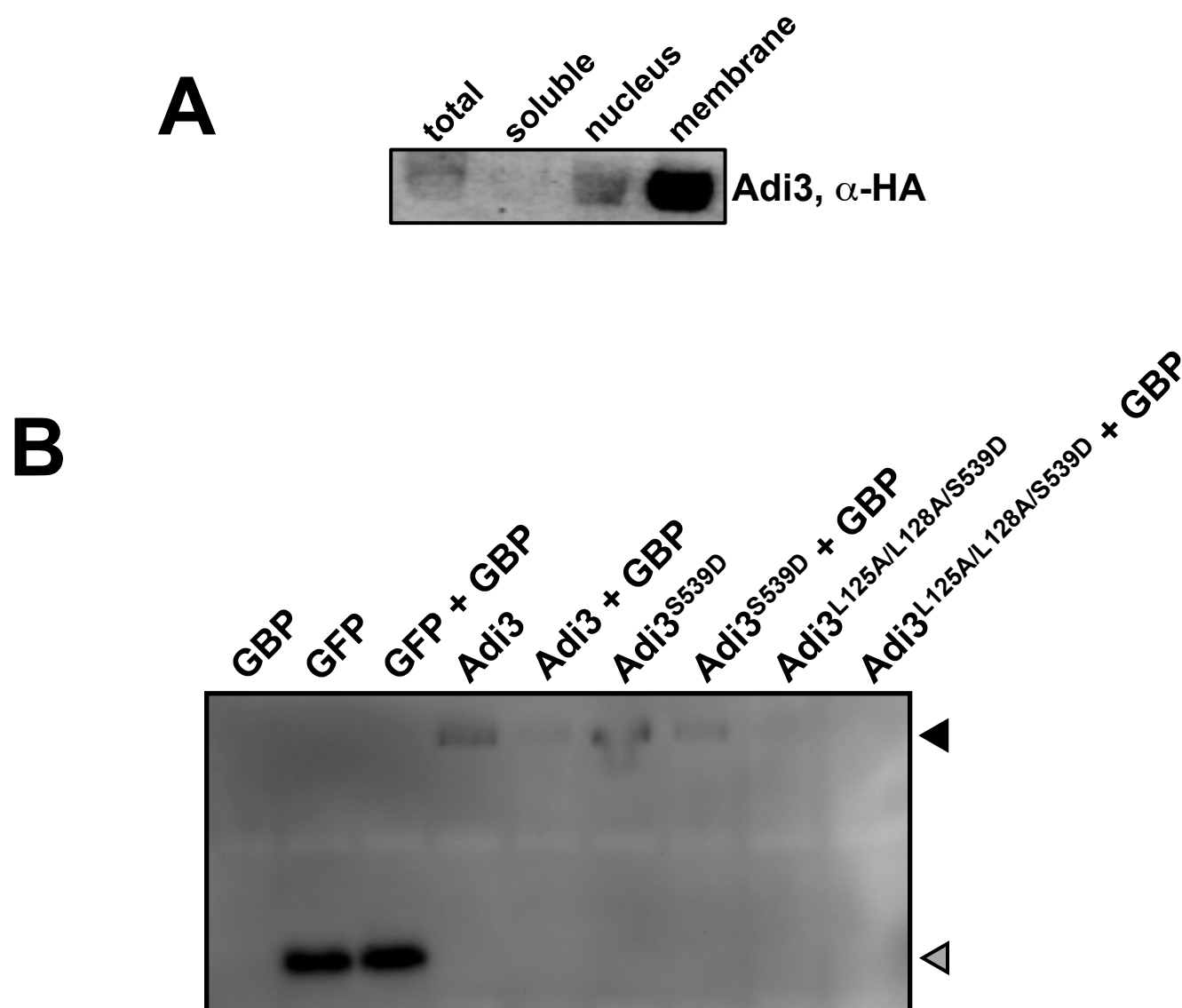
- Lam, E. (2004) *Nat. Rev. Mol. Cell Biol.* **5**, 305–315
- Greenberg, J. T., and Yao, N. (2004) *Cell Microbiol.* **6**, 201–211
- Mur, L. A., Kenton, P., Lloyd, A. J., Ougham, H., and Prats, E. (2008) *J. Exp. Bot.* **59**, 501–520
- Hoerichs, F. A., and Woltering, E. J. (2003) *Bioessays* **25**, 47–57
- Lam, E. (2008) *Crit. Rev. Plant Sci.* **27**, 413–423
- Jirage, D., Tootle, T. L., Reuber, T. L., Frost, L. N., Feys, B. J., Parker, J. E., Ausubel, F. M., and Glazebrook, J. (1999) *Proc. Natl. Acad. Sci. U.S.A.* **96**, 13583–13588
- Falk, A., Feys, B. J., Frost, L. N., Jones, J. D. G., Daniels, M. J., and Parker, J. E. (1999) *Proc. Natl. Acad. Sci. U.S.A.* **96**, 3292–3297
- Kachroo, P., Shanklin, J., Shah, J., Whittle, E. J., and Klessig, D. F. (2001) *Proc. Natl. Acad. Sci. U.S.A.* **98**, 9448–9453
- Liang, H., Yao, N., Song, J. T., Luo, S., Lu, H., and Greenberg, J. T. (2003) *Genes Dev.* **17**, 2636–2641
- Pedley, K. F., and Martin, G. B. (2003) *Annu. Rev. Phytopathol.* **41**, 215–243
- del Pozo, O., Pedley, K. F., and Martin, G. B. (2004) *EMBO J.* **23**, 3072–3082
- Bogdanove, A. J., and Martin, G. B. (2000) *Proc. Natl. Acad. Sci. U.S.A.* **97**, 8836–8840
- Devarenne, T. P., Ekengren, S. K., Pedley, K. F., and Martin, G. B. (2006) *EMBO J.* **25**, 255–265
- Vivanco, I., and Sawyers, C. L. (2002) *Nat. Rev. Cancer* **2**, 489–501
- Vara, J. A. F., Casado, E., de Castro, J., Cejas, P., Belda-Iniesta, C., and Gonzales-Baron, M. (2004) *Cancer Trt. Reviews* **30**, 193–204
- Bögge, L., Okrész, L., Henriques, R., and Anthony, R. G. (2003) *TRENDS Plant Sci.* **8**, 424–431
- Sobko, A. (2006) *Sci. STKE* 2006, re9
- Bivona, T. G., Quatela, S. E., Bodemann, B. O., Ahearn, I. M., Soskic, M. J., Mor, A., Miura, J., Wiener, H. H., Wright, L., Saba, S. G., Yim, D., Fein, A., Pérez de Castro, I., Li, C., Thompson, C. B., Cox, A. D., and Philips, M. R. (2006) *Mol. Cell* **21**, 481–493
- Cha, T. L., Zhou, B. P., Xia, W., Wu, Y., Yang, C. C., Chen, C. T., Ping, B., Otte, A. P., and Hung, M. C. (2005) *Science* **310**, 306–310
- Zegzouti, H., Anthony, R. G., Jahchan, N., Bögge, L., and Christensen, S. K. (2006) *Proc. Natl. Acad. Sci. U.S.A.* **103**, 6404–6409
- Zegzouti, H., Li, W., Lorenz, T. C., Xie, M., Payne, C. T., Smith, K., Glenny,

Adi3 Nuclear Localization Suppresses Cell Death

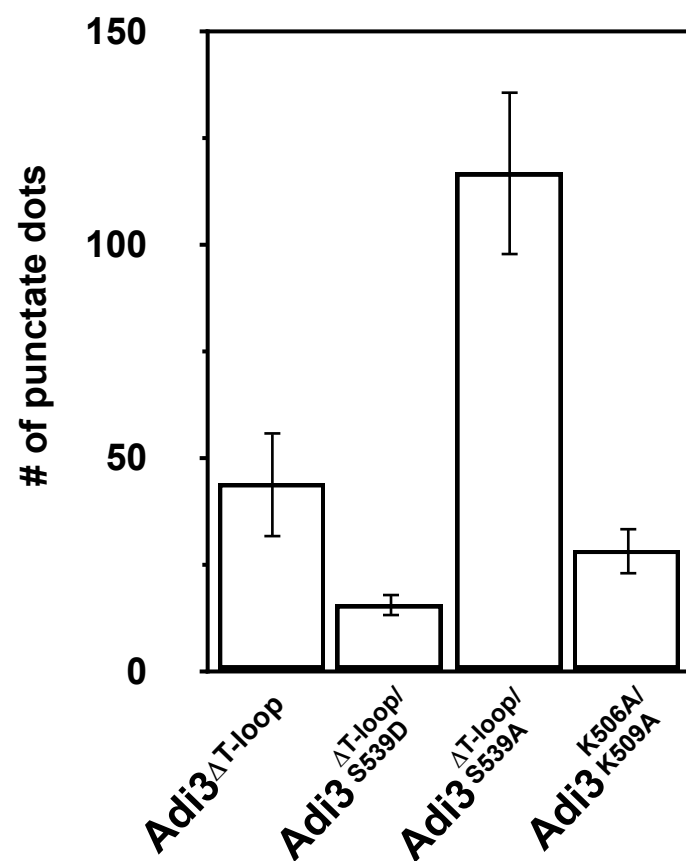
- S., Payne, G. S., and Christensen, S. K. (2006) *J. Biol. Chem.* **281**, 35520–35530
22. Anthony, R. G., Henriques, R., Helfer, A., Mészáros, T., Rios, G., Testerink, C., Munnik, T., Deák, M., Koncz, C., and Bögre, L. (2004) *EMBO J.* **23**, 572–581
 23. Anthony, R. G., Khan, S., Costa, J., Pais, M. S., and Bögre, L. (2006) *J. Biol. Chem.* **281**, 37536–37546
 24. Galván-Ampudia, C. S., and Offringa, R. (2007) *Trends Plant Sci.* **12**, 541–547
 25. Briggs, W. R., and Christie, J. M. (2002) *TRENDS Plant Sci.* **7**, 204–210
 26. Oyama, T., Shimura, Y., and Okada, K. (2002) *Plant J.* **30**, 289–299
 27. Rentel, M. C., Lecourieux, D., Ouaked, F., Usher, S. L., Petersen, L., Okamoto, H., Knight, H., Peck, S. C., Grierson, C. S., Hirt, H., and Knight, M. R. (2004) *Nature* **427**, 858–861
 28. Robert, H. S., and Offringa, R. (2008) *Curr. Opin. Plant Biol.* **11**, 495–502
 29. Hergovich, A., Cornils, H., and Hemmings, B. A. (2008) *Biochim. Biophys. Acta* **1784**, 3–15
 30. Tamaskovic, R., Bichsel, S. J., and Hemmings, B. A. (2003) *FEBS Lett.* **546**, 73–80
 31. Millward, T., Cron, P., and Hemmings, B. A. (1995) *Proc. Natl. Acad. Sci. U.S.A.* **92**, 5022–5026
 32. Bichsel, S. J., Tamaskovic, R., Stegert, M. R., and Hemmings, B. A. (2004) *J. Biol. Chem.* **279**, 35228–35235
 33. Higuchi, R., Krummel, B., and Saiki, R. K. (1988) *Nucleic Acids Res.* **16**, 7351–7367
 34. Haasen, D., Köhler, C., Neuhaus, G., and Merkle, T. (1999) *Plant J.* **20**, 695–705
 35. Nelson, B. K., Cai, X., and Nebenführ, A. (2007) *Plant J.* **51**, 1126–1136
 36. Horton, P., Park, K. J., Obayashi, T., Fujita, N., Harada, H., Adams-Collier, C. J., and Nakai, K. (2007) *Nucleic Acids Res.* **35**, W585–587
 37. Lee, C., Hodgins, D., Calvert, J. G., Welch, S. K., Jolie, R., and Yoo, D. (2006) *Virology* **346**, 238–250
 38. Meares, G. P., and Jope, R. S. (2007) *J. Biol. Chem.* **282**, 16989–17001
 39. Stommel, J. M., Marchenko, N. D., Jimenez, G. S., Moll, U. M., Hope, T. J., and Wahl, G. M. (1999) *EMBO J.* **18**, 1660–1672
 40. Chen, W. S., Xu, P. Z., Gottlob, K., Chen, M. L., Sokol, K., Shiyanova, T., Roninson, I., Weng, W., Suzuki, R., Tobe, K., Kadowaki, T., and Hay, N. (2001) *Genes Dev.* **15**, 2203–2208
 41. Lawlor, M. A., and Alessi, D. R. (2001) *J. Cell Sci.* **114**, 2903–2910
 42. Luo, H. R., Hattori, H., Hossain, M. A., Hester, L., Huang, Y., Lee-Kwon, W., Donowitz, M., Nagata, E., and Snyder, S. H. (2003) *Proc. Natl. Acad. Sci. U.S.A.* **100**, 11712–11717
 43. Dudek, H., Datta, S. R., Franke, T. F., Birnbaum, M. J., Yao, R., Cooper, G. M., Segal, R. A., Kaplan, D. R., and Greenberg, M. E. (1997) *Science* **275**, 661–665
 44. Arico, S., Patingre, S., Bauvy, C., Gane, P., Barbat, A., Codogno, P., and Ogier-Denis, E. (2002) *J. Biol. Chem.* **277**, 27613–27621
 45. Kulp, S. K., Yang, Y. T., Hung, C. C., Chen, K. F., Lai, J. P., Tseng, P. H., Fowble, J. W., Ward, P. J., and Chen, C. S. (2004) *Cancer Res.* **64**, 1444–1451
 46. Zhu, J., Huang, J. W., Tseng, P. H., Yang, Y. T., Fowble, J., Shiao, C. W., Shaw, Y. J., Kulp, S. K., and Chen, C. S. (2004) *Cancer Res.* **64**, 4309–4318
 47. Kudo, N., Khochbin, S., Nishi, K., Kitano, K., Yanagida, M., Yoshida, M., and Horinouchi, S. (1997) *J. Biol. Chem.* **272**, 29742–29751
 48. Kudo, N., Matsumori, N., Taoka, H., Fujiwara, D., Schreiner, E. P., Wolff, B., Yoshida, M., and Horinouchi, S. (1999) *Proc. Natl. Acad. Sci. U.S.A.* **96**, 9112–9117
 49. Rodin, S. A., Pis'menskii, V. F., Nikitin, A. M., Surovaya, A. N., and Gursky, G. V. (2001) *Dokl. Biochem. Biophys.* **379**, 235–238
 50. Böhm, C., Seibel, N. M., Henkel, B., Steiner, H., Haass, C., and Hampe, W. (2006) *J. Biol. Chem.* **281**, 14547–14553
 51. Seibel, N. M., Eljouni, J., Nalaskowski, M. M., and Hampe, W. (2007) *Anal. Biochem.* **368**, 95–99
 52. Rizhsky, L., Shulaev, V., and Mittler, R. (2004) in *Measuring Programmed Cell Death in Plants, Apoptosis Methods and Protocols* (Brady, H. J. M., ed) pp. 179–180, Humana Press, Totowa
 53. Schornack, S., Fuchs, R., Huitema, E., Rothbauer, U., Lipka, V., and Kamoun, S. (2009) *Plant J.* **60**, 744–754
 54. Salmeron, J. M., Barker, S. J., Carland, F. M., Mehta, A. Y., and Staskawicz, B. J. (1994) *Plant Cell* **6**, 511–520
 55. Salmeron, J. M., Oldroyd, G. E., Rommens, C. M., Scofield, S. R., Kim, H. S., Lavelle, D. T., Dahlbeck, D., and Staskawicz, B. J. (1996) *Cell* **86**, 123–133
 56. Madeo, F., Fröhlich, E., Ligr, M., Grey, M., Sigrist, S. J., Wolf, D. H., and Fröhlich, K. U. (1999) *J. Cell Biol.* **145**, 757–767
 57. Abramovitch, R. B., Kim, Y. J., Chen, S., Dickman, M. B., and Martin, G. B. (2003) *EMBO J.* **22**, 60–69
 58. Lam, E., Kato, N., and Lawton, M. (2001) *Nature* **411**, 848–853
 59. Ligterink, W., Kroj, T., zur Nieden, U., Hirt, H., and Scheel, D. (1997) *Science* **276**, 2054–2057
 60. Yang, K. Y., Liu, Y., and Zhang, S. (2001) *Proc. Natl. Acad. Sci. U.S.A.* **98**, 741–746
 61. Zhang, S., and Klessig, D. F. (2001) *Trends Plant Sci.* **6**, 520–527
 62. Ren, D., Yang, H., and Zhang, S. (2002) *J. Biol. Chem.* **277**, 559–565
 63. Li, S., Samaj, J., and Franklin-Tong, V. E. (2007) *Plant Physiol.* **145**, 236–245
 64. Kaneda, T., Taga, Y., Takai, R., Iwano, M., Matsui, H., Takayama, S., Isogai, A., and Che, F. S. (2009) *EMBO J.* **28**, 926–936
 65. Doukhanina, E. V., Chen, S., van der Zalm, E., Godzik, A., Reed, J., and Dickman, M. B. (2006) *J. Biol. Chem.* **281**, 18793–18801
 66. Scheid, M. P., Parsons, M., and Woodgett, J. R. (2005) *Mol. Cell Biol.* **25**, 2347–2363
 67. Miyamoto, S., Rubio, M., and Sussman, M. A. (2009) *Cardiovasc. Res.* **82**, 272–285
 68. Shiraishi, I., Melendez, J., Ahn, Y., Skavdahl, M., Murphy, E., Welch, S., Schaefer, E., Walsh, K., Rosenzweig, A., Torella, D., Nurzynska, D., Kajsztura, J., Leri, A., Anversa, P., and Sussman, M. A. (2004) *Circ. Res.* **94**, 884–891
 69. Adini, I., Rabinovitz, I., Sun, J. F., Prendergast, G. C., and Benjamin, L. E. (2003) *Genes Dev.* **17**, 2721–2732
 70. Lee, S. B., Xuan Nguyen, T. L., Choi, J. W., Lee, K. H., Cho, S. W., Liu, Z., Ye, K., Bae, S. S., and Ahn, J. Y. (2008) *Proc. Natl. Acad. Sci. U.S.A.* **105**, 16584–16589
 71. Xuan Nguyen, T. L., Choi, J. W., Lee, S. B., Ye, K., Woo, S. D., Lee, K. H., and Ahn, J. Y. (2006) *Biochem. Biophys. Res. Commun.* **349**, 789–798
 72. Biondi, R. M. (2004) *Trends Biochem. Sci.* **29**, 136–142
 73. Shan, L., Thara, V. K., Martin, G. B., Zhou, J. M., and Tang, X. (2000) *Plant Cell* **12**, 2323–2338



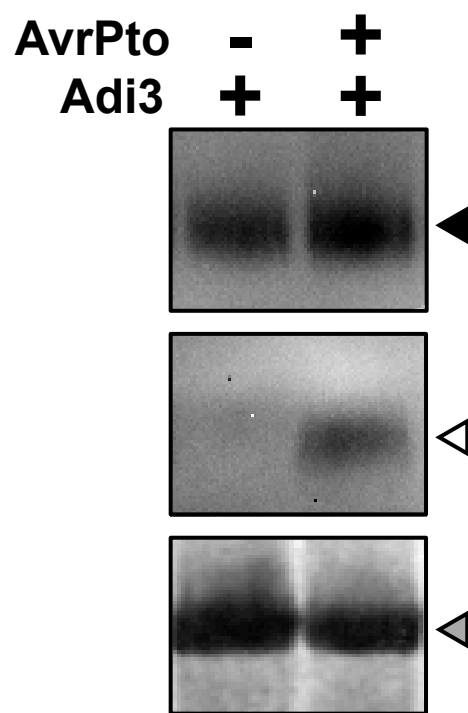
Supplemental Figure S1. **Detection of nonspecific protein band in α -GFP western blot.** The indicated proteins were expressed in PtoR tomato protoplasts for 16 hrs, total protein extracted, and 40 μ g of total protein analyzed by α -GFP western blot. A nonspecific protein band indicated by the asterisk can be detected in every sample including GFP alone and the empty vector. Filled triangle = GFP-Adi3 proteins; open triangle = GFP-Adi3 Δ T-loop proteins; gray triangle = GFP; asterisk = nonspecific protein; open diamond = RuBisCo loading control.



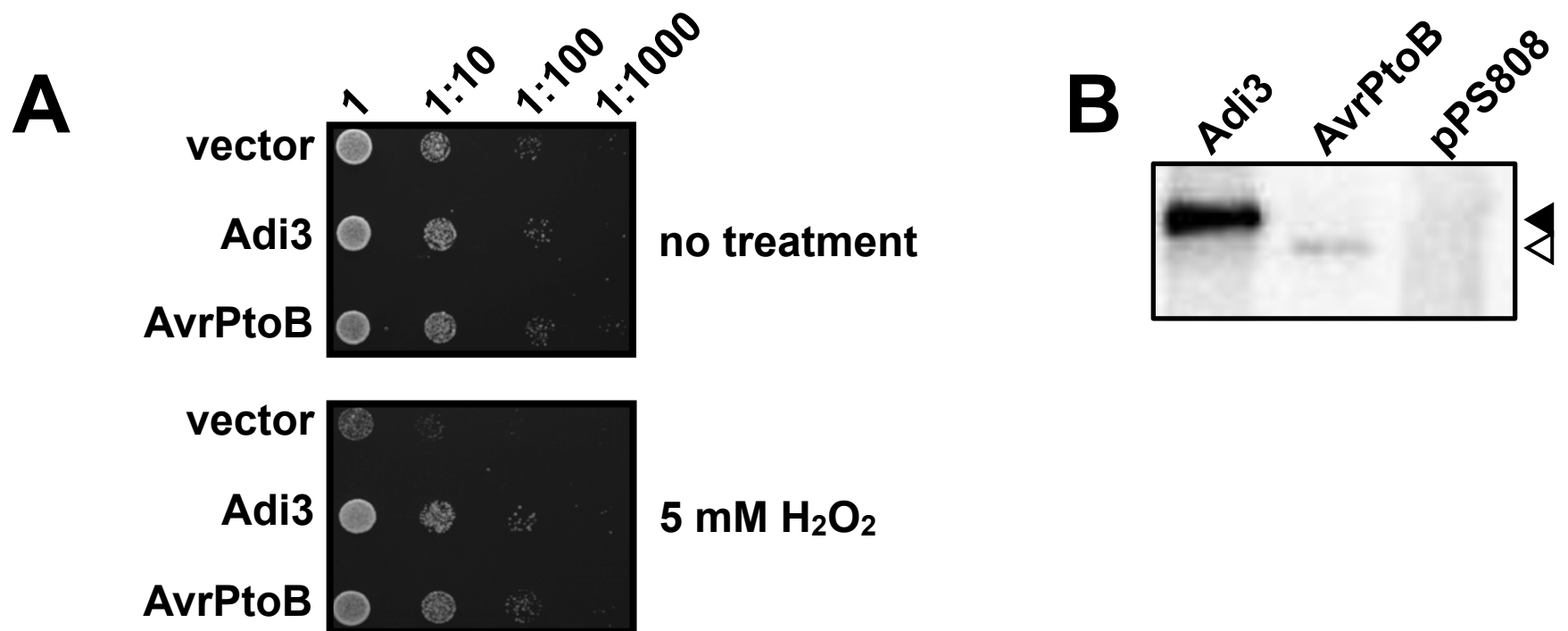
Supplemental Figure S2. **HA-Adi3 subcellular localization and reduction of GFP-Adi3 nuclear localization when expressed with GBP.** *A*, Western blot of cellular fractionation of HA-Adi3 expression in tomato protoplasts. Western blots were carried out with the α -HA antibody and are representative of three independent experiments. *B*, Reduction of nuclear GFP-Adi3 by GBP. The indicated proteins were expressed in tomato protoplasts for 16 hrs, nuclei isolated from each sample, and an α -GFP western blot carried out. The GBP protein is not capable of reducing GFP nuclear localization but does show a strong reduction of nuclear localized GFP-Adi3. The GBP protein does not have a GFP tag and thus is not detected in the western blot. Filled triangle = GFP-Adi3; gray triangle = GFP.



Supplemental Figure S3. **The number of punctate structures from deletion of the Adi3 T-loop extension.** The indicated *GFP-Adi3* constructs were expressed in tomato protoplasts for 16 hrs., viewed by confocal microscopy, and the number of GFP positive punctate structures counted in a minimum of three cells for each construct. The data from five independent experiments were averaged and shown with standard error.



Supplemental Figure S4. **Western blot detection of AvrPto expression after transformation of protoplasts transiently expressing Adi3.** PtoR protoplasts transiently expressing GFP-Adi3 for 14 hrs were transformed with a *BFP-avrPto* construct, proteins expressed for an additional 3 hrs, and the presence of Adi3 and AvrPto proteins analyzed by α -GFP western blot. Filled triangle = GFP-Adi3; open triangle = BFP-AvrPto, gray triangle = RuBisCo loading control.



Supplemental Figure S5. **Overexpression of Adi3 can suppress H₂O₂ cell death induction in yeast.** *A*, *GFP-Adi3* was expressed from the galactose inducible yeast expression vector pPS808 overnight at 30°C in the presence of glucose, switched to galactose media for 6 hrs, switched back to glucose media in the presence of 0 or 5 mM H₂O₂ for 2 hrs, and plated on YPD plates in serial dilutions. Galactose induced expression of the *Pst* effector protein GFP-AvrPtoB was used as a positive CDS control (48). *B*, Western blot detection (α -GFP) of Adi3 and AvrPtoB galactose induced yeast expression. Filled triangle, GFP-Adi3; open triangle, GFP-AvrPtoB.